Calculation of Magnetic Field and Optimization Design of High Field Magnet System with Ferromagnetic Shield

YANG Yandong[1], WANG Housheng[2]

1. *Economic and Technological Research Institute, Ningxia Electric Power Co., LTD. Yinchuan, Ningxia*, 753000, *P.R.China*;
2. *Key Laboratory of Applied Superconductivity, Institute of Electrical Engineering, Chinese Academy of Sciences, Beijing*, 100000, *P.R.China*

Received date: 2021-04-02; accepted date: 2022-01-28

【Abstract】 In this paper, an optimization design method for high field superconducting magnet with ferromagnetic shield is discussed. Firstly, the analytical formula for calculating the magnetic field at any space point is derived based on the equivalent magnetic charge model. Then the validity and accuracy of the formula are discussed by comparing the results with that of the finite element method (FEM) for the same model. Finally, a joint optimization of MRI magnet system with ferromagnetic shielding is carried out in order to improve the homogeneity of magnetic field in the DSV (diameter of spherical volum) region and enhance the field intensity in the center.

Keywords: ferromagnetic material, magnetic field calculation, high field magnet system, optimization design

PACS: 7460,7490,0290

DOI: 10.13380/j.ltpl.2022.01.008

Reference method: YANG Yandong, WANG Housheng, Low. Temp. Phys. Lett. **44**, 0089 (2022)

带铁磁屏蔽的高场磁体系统磁场计算与优化设计

杨彦东[1],王厚生[2]

1. 国网宁夏电力有限公司经济技术研究院 银川 753000;
2. 中科院电工所应用超导重点实验室 北京 100000

收稿日期:2021-04-02;接收日期:2022-01-28

【摘要】 本文提出了一种带铁磁屏蔽的高场超导磁体的优化设计方法.首先基于等效磁荷模型推导了空间中任意一点磁场强度的解析计算公式,然后与有限元方法计算结果相比较,验证了解析公式的准确性.最后,本文对一个带铁磁屏蔽的核磁共振磁体系统进行了联合优化设计,提高了中心磁场强度和均匀性.

关键词: 铁磁材料,磁场强度计算,高场磁体系统,优化设计

PACS: 7460,7490,0290

DOI: 10.13380/j.ltpl.2022.01.008

† mermaidyy@126.com

1 Introduction

In the designing of high field magnets for MRI, ferromagnetic materials are widely used for the shielding of leakage field so that equipment nearby will not be affected. In previous work, A. Ishiyama and H. Hirooka[1] adopted finite element and boundary-element method for the calculation of magnetic field of axially symmetric ferromagnetic materials and a mathematical programming method for solving the corre-sponding optimization problem. In the work of S. Noguchi and A. Ishiyama[2], they took equivalent magnetization current method to calculate the magnetic field, and the simulated annealing algorithm to solve corresponding optimization problem. Huawei Zhao and S. Crozier[3-5] derived the analytic for-mula of magnetic field generated by a circular ring of ferromagnetic material under arbitrary external magnetizing field. However, it seems that their formula didn't take into account the interaction between the magnetic rings, thus may not accurate in the calculation of magnetic field with nonlinear materials. Besides, the derivation process of their formulas may have some defects, we rededuce the formula of Huawei Zhao et al. and get a different form (see Appendix). Anyway, their formula is expressed as sum of infinite series rather than in-tegral, and is not convenient in use.

In fact, in all the researches above, the accuracy of the methods used to calculate the magnetic field intensity are not verified. In this paper, the analytical formula for calculating the magnetic field intensity at any space point is derived based on the equivalent magnetic charge model[6], which takes the nonlinear magnetic medium as the secondary field source. Then we compare the calculation results with that of the finite element method for the same model. After that we discussed the joint optimization methods for the designing of MRI magnet system with ferromagnetic shield.

2 Analytical formula for magnetic field

When the solution domain contains magnetic conductive medium, the equivalent magnetic charge modal regards the nonlinear medium as secondary field source:

$$\begin{cases} \vec{H} = \vec{H}_{\mathrm{f}} + \vec{H}_{\mathrm{m}} \\ \vec{B} = \vec{B}_{\mathrm{f}} + \vec{B}_{\mathrm{m}} \end{cases} \tag{1}$$

where vectors with subscript "f" and "m" represent the excitation field and the derivative field respectively.

According to Maxwell equations, the equations for excitation field and derivative field can be expressed as:

$$\begin{cases} \nabla \times \vec{H}_{\mathrm{f}} = \vec{\sigma}_{\mathrm{f}\tau} \\ \nabla \cdot \vec{B}_{\mathrm{f}} = 0 \\ \vec{B}_{\mathrm{f}} = \mu_0 \vec{H}_{\mathrm{f}} \\ (\vec{B}_{\mathrm{f1}} - \vec{B}_{\mathrm{f2}}) \cdot \vec{n}_0 = 0 \\ (\vec{H}_{\mathrm{f1}} - \vec{H}_{\mathrm{f2}}) \times \vec{n}_0 = \vec{\sigma}_{\mathrm{fs}} \\ \vec{H}_{\mathrm{f}}(r)\,|_{r\to\infty} = \vec{B}_{\mathrm{f}}(r)\,|_{r\to\infty} = 0 \end{cases} \tag{2}$$

$$\begin{cases} \nabla \times \vec{H}_{m} = 0 \\ \nabla \cdot \vec{B}_{\mathrm{m}} = -\mu_0 \nabla \cdot \vec{M} = \rho_{m\tau} \\ \vec{B}_{\mathrm{m}} = \mu_0 \vec{H}_{m} \\ (\vec{B}_{\mathrm{m1}} - \vec{B}_{\mathrm{m2}}) \cdot \vec{n}_0 = \rho_{ms} \\ (\vec{H}_{\mathrm{m1}} - \vec{H}_{\mathrm{m2}}) \times \vec{n}_0 = 0 \\ \vec{H}_{\mathrm{m}}(r)\,|_{r\to\infty} = \vec{B}_{m}(r)\,|_{r\to\infty} = 0 \end{cases} \tag{3}$$

where $\vec{\sigma}_{\mathrm{f}\tau}$ ($\vec{\sigma}_{\mathrm{fs}}$) represents the free volume (surface) current density distribution for the excitation field, and $\vec{\rho}_{\mathrm{m}\tau}$ ($\vec{\rho}_{\mathrm{m}s}$) denotes the equivalent magnetic volume (surface) charge for the derivative field.

Magnetization of the medium can be written as:

$$\vec{H}(P) = \frac{1}{\mu_r(P) - 1}\vec{M}(P) \tag{4}$$

where $\mu_r(P)$ is relative permeability of the medium at field point P.

When the magnetic conductive medium is dis-

sected into N equal units, the integral equation of the magnetization distribution inside of the medium can be expressed as[7]:

$$\frac{1}{\mu_r(i)-1}\vec{M}(i)=\frac{1}{4\pi}\sum_{j=1}^{N}\left\{\iiint_{\tau}-\nabla\cdot\vec{M}(j)\frac{\vec{r}_{ji}-\vec{r}_{jq}}{|\vec{r}_{ji}-\vec{r}_{jq}|^3}\mathrm{d}\tau+\iint_S\vec{M}(j)\cdot\vec{n}_0\frac{\vec{r}_{ji}-\vec{r}_{jq}}{|\vec{r}_{ji}-\vec{r}_{jq}|^3}\mathrm{d}S\right\}+\vec{H}_f(i),$$
$$i,j=1,2,\cdots,N \tag{5}$$

vectors $\vec{r}_i$ and $\vec{r}_j$ are coordinate vectors of the geo-metric centers of magnetization units "i" and "j" res-pectively, and $\vec{r}_{j^*}=\vec{r}^{\,*}-\vec{r}_j$, see Fig. 1.

For every magnetization units we set:

$$\lambda(i)=\frac{H(i)}{M(i)}=\frac{1}{\mu_r(i)-1},i=1,2,\cdots,N \tag{6}$$

We expect $M(i)=M^*(i)$, where $M^*(i)$ (see Fig. 2) is the coordinate of the intersection point of the straight line $M(i)=\lambda^{-1}(i)H(i)$ and the actual magnetization characteristic curve $M(i)=f(H(i))$, if $M(i)\neq M^*(i)$, then we need to fix the value of $\lambda(i)$ through:

$$\lambda(n+1)=\begin{cases}\lambda(n)\dfrac{M^+(n)}{f(\lambda(n)M^+(n))}\\ \lambda(n)\dfrac{M^-(n)}{f(\lambda(n)M^-(n))}\end{cases} \tag{7}$$

where $\lambda(n)$ is the initial value of the niteration, and $\lambda(n+1)$ the revised value. The coordinates of each point are P^*: (H^*,M^*), $Q^\pm$: $(\lambda(n)M^\pm(n),M^\pm(n))$, $P^\pm$: $(\lambda(n)M^\pm(n),f(\lambda(n)M^\pm(n))$

For a cylindrical symmetry system which is divided into magnetization rings along r-and z-direction as shown in Fig. 3, the discretization form of equation (5) write as:

$$\frac{1}{\mu_r(i)-1}\vec{M}(i)+\frac{1}{4\pi}\sum_{j=1}^{N}\{[\iiint_{\tau(j)}\frac{\vec{r}_i-\vec{r}_q(j)}{|\vec{r}_i-\vec{r}_q(j)|^3}\mathrm{d}\tau]M_\rho(j)-[\iint_{S_{r+(j)}}\frac{\vec{r}i-\vec{r}_q(j)}{|\vec{r}_i-\vec{r}_q(j)|^3}\mathrm{d}S-\iint_{S_{r-(j)}}\frac{\vec{r}_i-\vec{r}_q(j)}{|\vec{r}_i-\vec{r}_q(j)|^3}\mathrm{d}S]M_\rho(j)+[\iint_{S_{z+(j)}}\frac{\vec{r}_i-\vec{r}_q(j)}{|\vec{r}_i-\vec{r}_q(j)|^3}\mathrm{d}S-\iint_{S_{z-(j)}}\frac{\vec{r}_i-\vec{r}_q(j)}{|\vec{r}_i-\vec{r}_q(j)|^3}\mathrm{d}S]M_z(j)\}=\vec{H}_f(i) \tag{8}$$

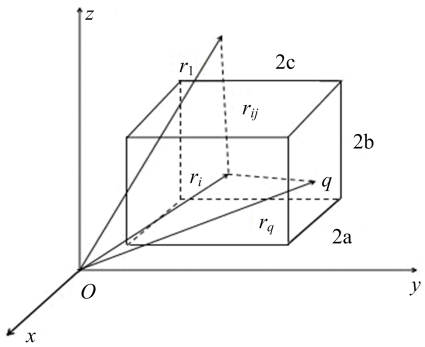

Fig. 1 Dissection of equal magnetization units

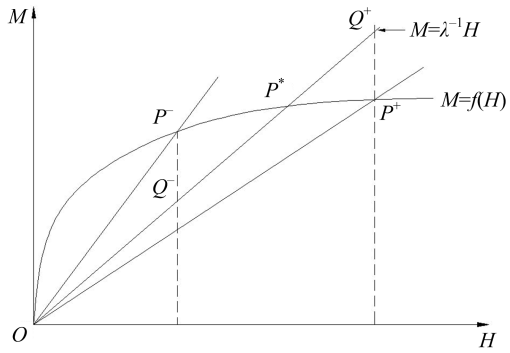

Fig. 2 Nonlinear magnetization characteristic of the ferromagnetic material

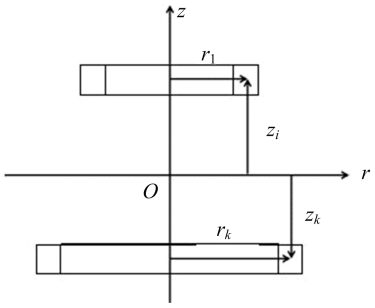

Fig. 3 Dissection of magnetization ring in cylindrical symmetry system

where $\vec{r}_q(j)$ is the vector of movement point "q" in the "j" unit, in zy lindrical coordinate system we write:

$$\vec{r}_i-\vec{r}_q(j)=(r_i-r_q(j)\cos\phi)\vec{e}_x-r_q(j)\sin\phi\vec{e}_y+(z_i-z_q(j))\vec{e}_z \tag{9}$$

where

$$\begin{cases}\mathrm{d}\tau=\rho_q d\varphi d\rho_q dz_q\\ \mathrm{d}S_R=(r_j\pm a(j))d\varphi dz_q\\ \mathrm{d}S_z=r_q d\varphi dr_q\end{cases} \tag{10}$$

Substitute eq. (9) and (10) into eq. (8), the radial and axial components of the magnetic field can be written as a column matrix, when field point "p" is outside the magnetic medium:

$$\begin{pmatrix} [H_r(p)] \\ [H_z(p)] \end{pmatrix} = \begin{pmatrix} [\xi_{rr}(p,j)] & [\xi_{rz}(p,j)] \\ [\xi_{zr}(p,j)] & [\xi_{zz}(p,j)] \end{pmatrix} \begin{pmatrix} [M_r(j)] \\ [M_z(j)] \end{pmatrix} + \begin{pmatrix} [H_{fr}(p)] \\ [H_{fz}(p)] \end{pmatrix} \tag{11}$$

where $[\xi_{**}(p,j)]$ and $[M_*(j)]$ are n-dimensional row and column vectors respectively. Inside of the magnetic medium, it writes:

$$\begin{pmatrix} [H_r(p)] \\ [H_z(p)] \end{pmatrix} = \left[\frac{1}{\mu_r(p)-1}\right] \begin{pmatrix} [M_r(j)] \\ [M_z(j)] \end{pmatrix} \tag{12}$$

the coefficients above are determined by:

$$\xi_{rr}(i,j) = \frac{1}{2\pi}\sum_{k=1}^{4}(-1)^k \int_0^{\pi} \left\{ \frac{-r_k \cdot z_k(r_i - r_k\cos\varphi)}{(r_i^2 + r_k^2 - 2r_i \cdot r_k\cos\varphi)\sqrt{r_i^2 + r_k^2 + z_k^2 - 2r_i \cdot r_k\cos\varphi}} + \right.$$
$$\sin\varphi \arctan \frac{z_k(r_k - r_i\cos\varphi)}{r_i\sin\varphi\sqrt{r_i^2 + r_k^2 + z_k^2 - 2r_i \cdot r_k\cos\varphi}} -$$
$$\left. \cos\varphi \cdot \ln\left[-z_k + \sqrt{r_i^2 + r_k^2 + z_k^2 - 2r_i \cdot r_k\cos\varphi}\right] \right\} d\varphi \tag{13}$$

$$\xi_{zz}(i,j) = \frac{1}{2\pi}\sum_{k=1}^{4}(-1)^k \int_0^{\pi} \frac{-z_k(r_i^2 + z_k^2 - r_i \cdot r_k\cos\varphi)}{(r_i^2\sin^2\varphi + z_k^2)\sqrt{r_i^2 + r_k^2 + z_k^2 - 2r_i \cdot r_k\cos\varphi}} d\varphi \tag{14}$$

$$\xi_{rz}(i,j) = \frac{1}{2\pi}\sum_{k=1}^{4}(-1)^k \int_0^{\pi} \left\{ \frac{r_i^2\sin^2\varphi(2r_k\cos\varphi - r_i) + z_k^2(r_k\cos\varphi - r_i\sin^2\varphi)}{(r_i^2\sin^2\varphi + z_k^2)\sqrt{r_i^2 + r_k^2 + z_k^2 - 2r_i r_k\cos\varphi}} - \right.$$
$$\left. \cos\varphi \cdot \ln\left[r_k - r_i\cos\varphi + \sqrt{r_i^2 + r_k^2 + z_k^2 - 2r_i \cdot r_k\cos\varphi}\right] \right\} d\varphi \tag{15}$$

$$\xi_{zr}(i,j) = \frac{1}{2\pi}\sum_{k=1}^{4}(-1)^k \int_0^{\pi} \left\{ \frac{r_k}{\sqrt{r_i^2 + r_k^2 + z_k^2 - 2r_i \cdot r_k\cos\varphi}} - \right.$$
$$\left. \ln\left[r_k - r_i\cos\varphi + \sqrt{r_i^2 + r_k^2 + z_k^2 - 2r_i \cdot r_k\cos\varphi}\right] \right\} d\varphi \tag{16}$$

where r_k and z_k take the following values:

Tab. 1 r_k and z_k for different k values

k	1	2	3	4
r_k	$r_j + a(j)$	$r_j + a(j)$	$r_j - a(j)$	$r_j - a(j)$
z_k	$z_i - z_j + c(j)$	$z_i - z_j - c(j)$	$z_i - z_j - c(j)$	$z_i - z_j + c(j)$

3 Treatment of singularities

It's important to note that there are some cases when singularities emerge in the coefficients above:

Case 1: $\varphi \to 0, r_i = r_k, z_k \neq 0, (i \neq k)$

Leads to: $\xi_{rr}(i,j) \to \infty$

Case 2: $\varphi \to 0, r_i \neq r_k, z_k = 0, (i \neq k)$

Leads to: $\xi_{zz}(i,j) \to \infty$

Case 3: $\varphi \to 0, r_i = r_k, z_k = 0$

Leads to: $\xi_{zr}(i,j) \to \infty$ and $\xi_{rz}(i,j) \to \infty$

The methods we take to treat singularities is different from that of [8], we assign rings in the same layer along the r-direction with the same radial parameter, by which we could avoid $r_i = r_k$ $(i \neq k)$. Since parameters with different subscripts have increments other than zero (see table 1), if we divide the cylinder into proper layers (depending on the way we assign the initial values) along z-direction, then the case $z_k = 0$ will be avoided too.

We compare the results of two different calculation methods for the magnetic field of the same model, as shown in Fig. 4 and Fig. 5.

The parameters of the cylindrical iron screen are set as follows: inner diameter 1.0 m, outer diameter 1.5 m, Z-axis coordinate [−1,1]. When calculation is carried out with analytical method, the iron screen is divided into 11×77 (r-direction ×z-direction).

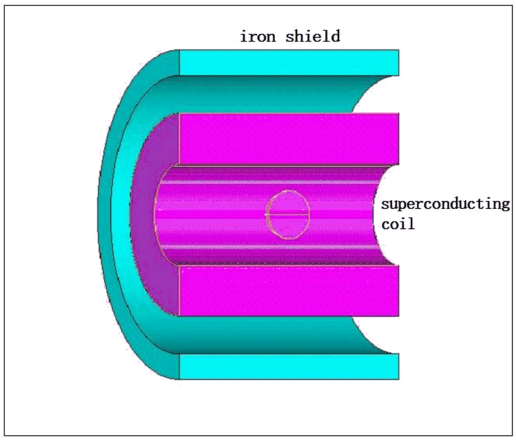

Fig. 4 Nonlinear magnetization characteristic of the ferromagnetic material

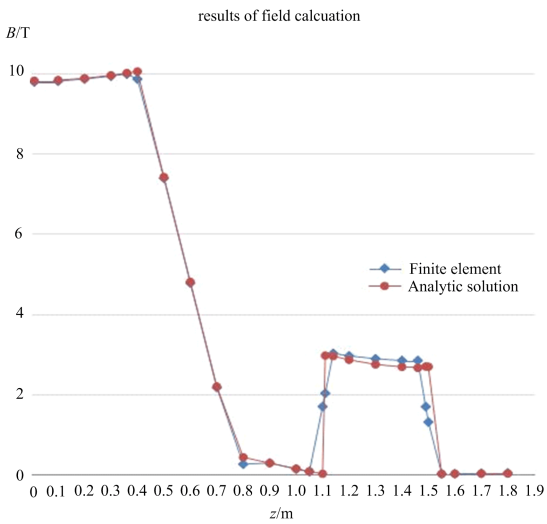

Fig. 5 Analysis of the results of field calculation in z-direction by two different methods

The magnetic field of axial symmetrical current-carrying coils was calculated by the Biot-Savart law, and the Gauss-Legendre 24-node numerical integration method was adopted for the calculation of the integral[9]. The initial layout of our superconducting coils was determined by the current density mapping method (CDM)[10, 11]. When calculation is carried out with finite element method, we adopt the edge element-based magnetic vector potential method, in which a 20-node hexahedron element is used in the element section, and there is an edge flux degree of freedom at the middle node of each edge. Element size of coils is set as 0.04 m, that of ferromagnetic material and air is 0.1 m. In order to meet engineering needs, the convergence criteria is 10^{-10} up to 30 equilibrium iteration. Nonlinear magnetization characteristics of magnetic medium was considered through a nonlinear iterative method[7].

As shown in Fig. 5, The results of the two methods are very close in most regions except for that of the ferromagnetic area.

Here we proposed that, when calculation is conducted with finite element method, there is an accuracy lost on the interface of materials with different permeability[12] based on the fact that the normal components of the magnetic vector is very large on the interface, thus affects the computational accuracy.

Beyond magnetic conductive areas, the results of both methods are highly reliable. However, when we have to consider the rotation of the model and con-struction error, the model needs to be further refined, which makes the modeling more difficult for the analytical method, then it is more convenient to use FEM for modeling and optimization. Because of the convenience of finite element method in complex model building and meshing, we take 3D finite element analysis, combined with computer search techniques for our optimization process. At last, due to the accuracy lost on the interface of materials by the FEM, it is necessary to use analytical method to verify and analyze the calculation results.

4 Optimization design of MRI magnet system

In our optimization task for a 9.4 T MRI magnet system, we aim to keep the magnetic field intensity in the center of DSV (diameter of spherical volum) between 9.45 T and 9.46 T, while increasing the uniformity of field in DSV region as much as possible. In addition, the range of

5 G lines (1 G = 1 Gauss = 10^{-4} Tesla) should be limited within 6.5 m from the center of DSV. The objective function is defined as:

$$Z = \omega_1 \cdot (B_0 - B_{obj}) + \omega_2 \sum_{j=1}^{m} (d_j^- + d_j^+) + \omega_3 \sum_{j=1}^{l} D_z \tag{17}$$

$$0 \leqslant \{|J_i|\} \leqslant J_{\max}, i = (1,2,3,\cdots,n) \tag{18}$$

where B_0 represents the field intensity of the center of DSV region; d_j^+ and d_j^- are positive and negative bias variables; $\omega_i (i = 1,2,3)$ are weight coefficients; l and m are the number of control nodes that constrain the magnetic field intensity; D_z is the distant of 5-G lines from the center of DSV region in z-direction; Constraint (18) taking into account of the H-I characteristics of superconducting material, where J_i are current density of superconducting coils.

Now consider the applicability of some common optimization algorithms:

Sequential quadratic programming (SQP) method[13] is mainly applied to problems with smooth continuously differentiable objective function and constraints, which has poor global optimization ability for multi-variable problems.

Simulated annealing algorithm is a random search method, which is a general and effective approximation algorithm suitable for solving large-scale combination optimization problems, and does not depend on the choice of initial conditions. However, as pointed out by G. Drago[14], the convergence rate of the simulated annealing algorithm in the later stage of optimization is also a problem worth considering.

Multi-objective particle swarm[15, 16] is widely used in the process of optimization which involves multi-variable, multi-constraint and multi-objective problems, which has a strong parallel search ability and good converging ability for complex optimization problems with multiple variables.

Multi-islands genetic[17,18] is essentially a random search algorithm, which has a strong parallel search ability and good converging ability for complex optimization problems with multiple variables.

By comparing several optimization algorithms, we select multi-objective particle swarm method, which shows a strong multi-peak optimization ability.

Optimization process takes several steps, firstly, the main magnetic body parameters are optimized within a wide range as a linear global optimization problem, then the geometry parameters of main magnetic body and the ferromagnetic shield are cooptimized as a non-linear local optimization problem. Then the final model is dissected more finely and recalculated to ensure the accuracy and ready for further optimization. The optimization results are shown in Fig. 6～Fig. 7.

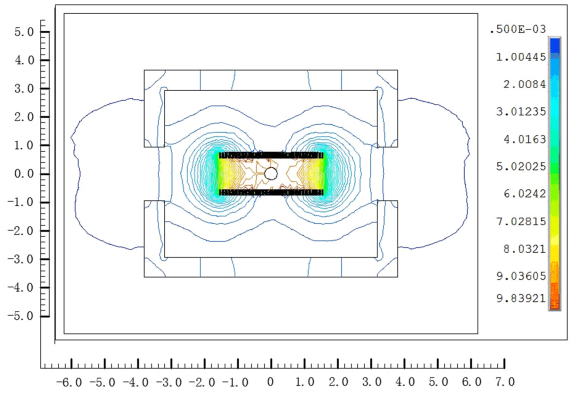

Fig. 6 Magnetic field intensity contours before optimization

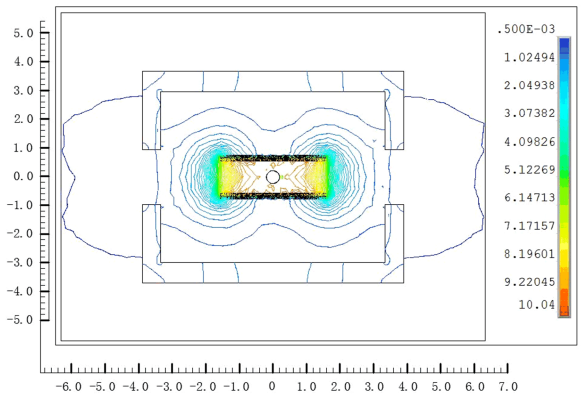

Fig. 7 Magnetic field intensity contours after optimization

The homogeneity of field in the DSV region

hasim-proved from 4600 ppm to 200 ppm over a DSV of 38 cm in diameter, and reaches 9.4538 T in the center of DSV region and ready for shimming design in the next. To give priority to uniformity of field in DSV region, the range of 5G lines enlarged from 5.99 m to 6.24 m, which is an acceptable sacrifice.

5 conclusion

In this paper, an effective way for solving com-plicated nonlinear optimization problems has been proposed, during which the validity and accuracy of the analytical formula for calculating the magnetic field is discussed by comparing the results with that of the finite element method. The approach we adopted here is proved to be feasible, and can be readily spread to solve geometrical and structural optimization problems in other engineering areas.

6 Acknowledgment

The authors would like to thank ProfessorYinming Dai, Qiuliang Wang and Dr. Yi Li for their instructive advice and useful suggestions on this thesis.

Appendix

We re-deduce formulas (19) and (20) in literature[4], here we only give the final results of our deduction:

$$B_{mr}=\begin{cases}\dfrac{\mu_0}{r_0^2}\sum_{n=0}^{\infty}\left(\dfrac{r}{r_0}\right)^{n+1}P_{n+1}^1(\cos\theta)[(n+3)P_{n+3}(\cos\alpha)M_z+P_{n+3}^1(\cos\alpha)M_r],\ (r<r_0)\\ \dfrac{\mu_0}{r^2}\sum_{n=0}^{\infty}\left(\dfrac{r_0}{r}\right)^{n+1}P_{n+2}^1(\cos\theta)[-(n+1)P_n(\cos\alpha)M_z+P_n^1(\cos\alpha)M_r],\ (r>r_0)\end{cases}\tag{19}$$

$$B_{mz}=\begin{cases}\dfrac{\mu_0}{r_0^2}\sum_{n=0}^{\infty}(n+1)\left(\dfrac{r}{r_0}\right)^{n}P_n(\cos\theta)[(n+2)P_{n+2}(\cos\alpha)M_z+P_{n+2}^1(\cos\alpha)M_r],\ (r<r_0)\\ \dfrac{\mu_0}{r^2}\sum_{n=0}^{\infty}\left(\dfrac{r_0}{r}\right)^{n+1}P_{n+2}(\cos\theta)[(n+1)(n+2)P_n(\cos\alpha)M_z-P_n^1(\cos\alpha)M_r],\ (r>r_0)\end{cases}\tag{20}$$

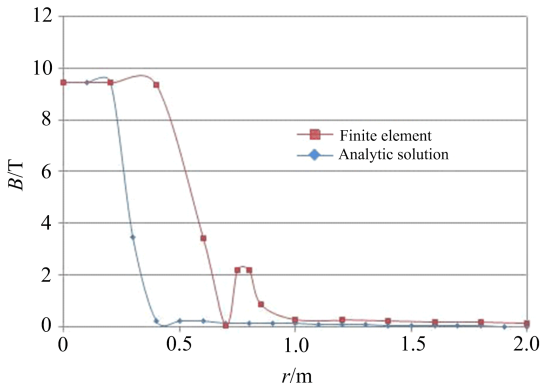

Fig. 8 Comparison of results: distribution of magnetic field at $z=0$ m by two different methods

where

$$M_r=(1/2)ds\cdot r_0\sin^2\alpha\frac{\chi_r B_\rho}{(\chi_r+1)}$$

$$M_z=(1/2)ds\cdot r_0\sin^2\alpha\frac{\chi_z B_z}{(\chi_z+1)}$$

χ_r and χ_z are magnetic susceptibility in r-and z-direction respectively.

The calculation results for the same modal in our paper according to eq. (19) and (20) are shown in Fig. 8. We do not get the expected results as that in Fig 5, the methods proposed in ref. [4-6] for the calculation of magnetic field with iron shielding is doubt worthy.

In addition, their formula is expressed as sum of infinite series rather than an integral, and how to control the accuracy of the formula is also a problem worth consideration.

Reference

[1] A. Ishiyama and H. Hirooka, *IEEE Trans. Magn.*, **27** (1991),1692.

[2] S. Noguchi and A. Ishiyama, *IEEE Trans. Magn.*, **32** (1996), 2655.

[3] H. Zhao, S.. Crozier and D. M. Doddrell, *J. Magn. Reson.*, **141** (1999), 340.

[4] H. Zhao and S. Crozier, *Meas. Sci. Technol.*, **13** (2002),198.

[5] H. Zhao and S. Crozier, *Concepts Magn. Reson.*, **15** (2000), 208.

[6] L. K. Forbes, S. Crozier, and D. M. Doddrell, *IEEE Trans. Magn.*, **33** (1997), 4405.

[7] Z. Feng and S. Han, *Trans. China Electrotech. Soc.*, **3** (1990),06.

[8] Z. X. Feng, *IEEE Trans. Magn.*, **21** (1985), 2207.

[9] 雷银照. 轴对称线圈磁场计算[M]. 中国计量出版社, 1991.

[10] C. J. Snape-Jenkinson, L. K. Forbes, and S. Crozier, *IEEE Trans. Magn.*, **35**(1999), 4159.

[11] L. K. Forbes and S. Crozier, *IEEE Trans. Magn.*, **33** (1997), 4405.

[12] O. Biro, K.. Preis, and K. R. Richter, *IEEE Trans. Magn.*, **32**(1996), 651.

[13] N. Hu, P. Zhou, and J. Yang, *Energy Convers. Magn.* **133** (2017),138.

[14] G. Drago, A. Manella, M. Nervi, M. Repetto, and G. Secondo, *IEEE Trans. Magn.*, **28**(1992), 1541.

[15] X. Yan and H. Shi, *Seventh International Confer-ence on Natural Computation*, Shanghai, China, 26-28 July, (2011).

[16] L. Yang, *The 2008 IEEE International Conference on Granular Computing*, GrC 2008, Hangzhou, China, 26-28 August, 2008.

[17] W. Zhou and J. Lu, *Ship Engineering*, **5**(2014), 46.

[18] A. Guillén, I. Rojas, J. González, H. Pomares, and B. Paechter, *Proceedings of the 19th Australian joint conference on Artificial Intelligence: advances in Artificial Intelligence*, (2008).

[19] H. Yu, *Acta Phys. Sin-ch ed*, **63**(2014), 294.